

INFLUENCE OF ABSORBER LAYER GRADUAL GAP PROFILE ON $\text{Cu}_2\text{ZnSn}(\text{S}_{1-y}\text{Se}_y)_4$ SOLAR CELL EFFICIENCY: NUMERICAL STUDY

N. Messei

Laboratory of thin films and applications “LPCM”, Mohamed Khider University,
BP, 07000 Biskra, Algeria

Received: 26 April 2020 / Accepted: 28 October 2020 / Published online: 01 January 2021

ABSTRACT

The gradual substitution of sulfur atoms (S) by selenium atoms (Se) in $\text{Cu}_2\text{ZnSn}(\text{S}_{1-y}\text{Se}_y)_4$ compounds causes a linear increase in the optical band-gap. For this reason, those compounds are suitable to implement band-gap engineering in compositionally graded solar cells. In this paper, we have worked to take advantage of this feature to enhance the performances of the basic uniform Kesterite and Stannite CZTS $_{1-y}$ Se $_y$ solar cells. The influence of two grading profiles was investigated: fully graded (a) and double graded (b). Fully graded Cell showed better parameters than compositionally uniform cells. In Double graded cells it appeared that front grading had a disruptive effect on solar cell parameters. In contrary back grading ameliorates significantly all cell parameters. As a result, the efficiency of kesterite and stannite cells was enhanced from 9.05 and 5.22% to 16.65 and 15.77 % respectively.

Key words: CZTS $_{1-y}$ Se $_y$; Kesterite; Stannite; thin film; solar cell; graded; SCAPS 1D.

Author Correspondence, e-mail: nadia.messei@univ-biskra.dz

doi: <http://dx.doi.org/10.4314/jfas.v13i1.20>

1. INTRODUCTION

The increase of energy prices has increased the attention to renewable energies significantly, in particular photovoltaics. The Rapid development of Thin-film technology still offers the possibility of reducing solar cell manufacturing costs. However, most of the materials used in the production of thin film absorber contain either rare or toxic elements. Nowadays, the

quaternary p-type semiconductors $\text{Cu}_2\text{ZnSnSe}_4$ (CZTSe) , $\text{Cu}_2\text{ZnSnS}_4$ (CZTS) and their alloys $\text{Cu}_2\text{ZnSn}(\text{S}_{1-y}\text{Se}_y)_4$ (CZTSSe) with direct band gap between 0.7 and 1.5 eV has particularly attracted attentions[1,2]. Those materials are derived from CuInGaSe_2 (CIGS) and keep its noticeable photovoltaic properties, but also contains earth abundant and safe elements like Zn and Sn. The pre-factor of absorption coefficient for the CZTSSe thin film is large enough ($>10^4\text{cm}^{-1}$), in other word the absorber of just micron thickness is able to absorb sunlight sufficiently, without any damaging effects on photocurrents.

For CZTSSe compounds, different crystal structure types are discussed in the literature, including the kesterite-type and the stannite-type structures. Both structures are closely related, but show a different cation distribution which leads to different space groups. The kesterite-type structure is characterized by alternating cation layers of CuSn, CuZn, CuSn, and CuZn at $z=0, 1/4, 1/2,$ and $3/4,$ respectively [3]. while in the stannite-type structure ZnSn layers alternate with Cu_2 layers [3]. in literature, there is no compelling evidence that any macroscopic CZTSSe sample produced to date is actually 100% kesterite or 100% stannite [4], however most published works focused on kesterite CZTSSe solar cell [5,6]. Stannite CZTSSe alloys solar cell needs to be investigated.

Despite The discovery that a CZTS thin film has an optimum direct band-gap of 1.45eV for solar cells was made in1988 in the laboratory of Shinshu University [7], the efficiency of CZTSSe solar cells remains under devices of absorber layer produced from older materials such as CIGS (η % 20.4%), CdTe (η % 19.6%) and GaAs (η % 28.8%) [8]. The current highest photoelectric conversion efficiency of CZTSe and CZTS based solar cells is 12.6% [9] and 8.5% [10] respectively, this efficiency is very low compared to its theoretical limit (> 32 %), according to Shockley-Queisser photo balance calculations [11]. To increase the conversion efficiency of CZTSSe solar cell, several optimization techniques have been proposed. Usually, in uniform solar cell, the band gap energy E_g of the absorber material is optimized by the well-known exchange between high current for low E_g and high voltage for high E_g . To achieve further increase in the efficiency, we applied a gradual gap profile ($E_g(x)$) across the absorber layer (in the direction x). This can be achieved by using a compositional graded absorber. Thus, most materials properties of the absorber layer will gradually change in the same direction. The idea is, to increase the short circuit current density J_{sc} while maintaining the open circuit voltage V_{oc} by realizing a well-suited band gap profile $E_g(x)$. K. Woo & all reports that high J_{sc} and less loss of V_{oc} are attributed to the effect of band gap grading induced by Se grading in the CZTSSe absorber layer [12].

2. UNIFORM OR GRADED ABSORBER?

In uniform layer, the driving forces for electrical current are, the electrostatic potential gradient $\nabla\Phi$ (drift current) and the concentration gradients ∇n and ∇p (diffusion current). When grading is present, additional driving terms should be added: the gradient of the band gap ∇E_g , the gradient of the electron affinity $\nabla\chi$, and the gradients of the effective density of states in the conduction $\nabla(\log N_C)$ and valence bands $\nabla(\log N_V)$. Furthermore, the electron and hole continuity equations are modified by the presence of a mobility gradient $\nabla\mu_n$ or $\nabla\mu_p$ (eq.(1)) and the Poisson equation is modified by a gradient $\nabla\varepsilon$ in dielectric constant (eq.(2)). These revised equations have been described in the literature [13] [14], and are implemented in the simulation package used in this work (SCAPS 1D) [14].

$$\frac{dn}{dt} = \mu_n \frac{1}{q} \frac{d^2 E_{Fn}}{dx^2} + \frac{1}{q} \frac{d\mu_n}{dx} \frac{dE_{Fn}}{dx} + G(x) + R(x) \quad (1)$$

$$\varepsilon \frac{d^2 \Phi}{dx^2} + \frac{d\varepsilon}{dx} \frac{d\Phi}{dx} = -\frac{\rho(x)}{\varepsilon_0} \quad (2)$$

In literature, several grading profiles were proposed for several materials like AlGaAs and CIGS. In this paper we have investigated two grading profiles (a) and (b) as shown in fig.1. In profile (a), the absorber was fully graded from the back to the front, in other words, the absorber begins with large band gap material and finishes with low band gap material. Experimentally, profile (a) enhances the cell efficiency by enhancing J_{sc} as reported in ref [12]. In order to obtain the profile (b) the absorber layer is divided into three layers [16]: in the first layer the band-gap decreases from E_{g1} to E_{g2} , remains unchanged in the second layer and increases from E_{g2} to E_{g3} in the third layer.

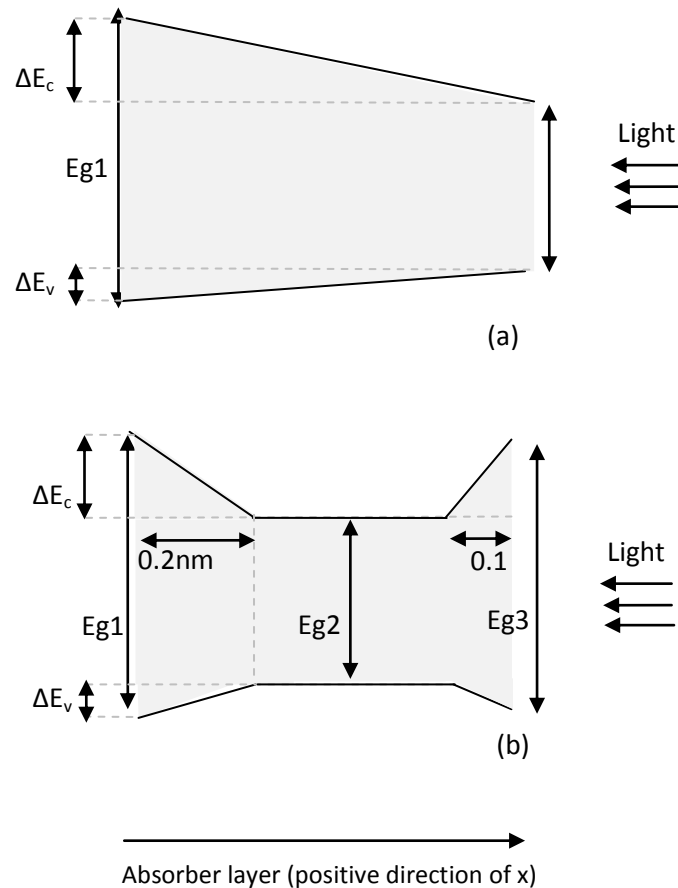


Fig.1. a Schematic diagram of band alignment in Se-graded CZTSSe absorber layer. The increase of E_g is mainly caused by increase of the CBO: (a) fully graded absorber layer, (b) double graded absorber layer

3. SIMULATION PROCESS

3.1. Numerical simulation program

The simulation has been carried out using the simulation package, SCAPS 1D, a one-dimensional solar cell device simulator developed at *Electronics and Information Systems (ELIS)*, University of Gent [16]. From version 2.8 onward, SCAPS 1D also implements graded solar cells [15]. A variety of interpolation laws are available to set the position dependent composition y of each layer: $y(x)$. These interpolation laws can also be applied to set the composition dependence of all relevant semiconductor properties in a layer, the most relevant properties are the band-gap $E_g(y)$ and the electron affinity $\chi(y)$. So, the combination with the composition profile $y(x)$ gives the ‘grading’ of these parameters, e.g. $E_g(x) = E_g[y(x)]$. In fact, the grading of up to eighteen properties can be set.

3.2. General device parameters

In this study, we consider the schematic structure of CZTS (CZTSe) solar cell commonly used [18, 19, 12] as shown in Fig.2. In which 1 μm p-CZTSe film, 70 nm n-CdS film, 50 nm i-ZnO and 200 nm n+(ZnO) are successively grown. Highly doped ZnO layer is necessary to collect charge carriers from the thin-film solar cell. In this work, the uniform absorber layer will be replaced by a graded CZTS_(1-y)Se_y layer.

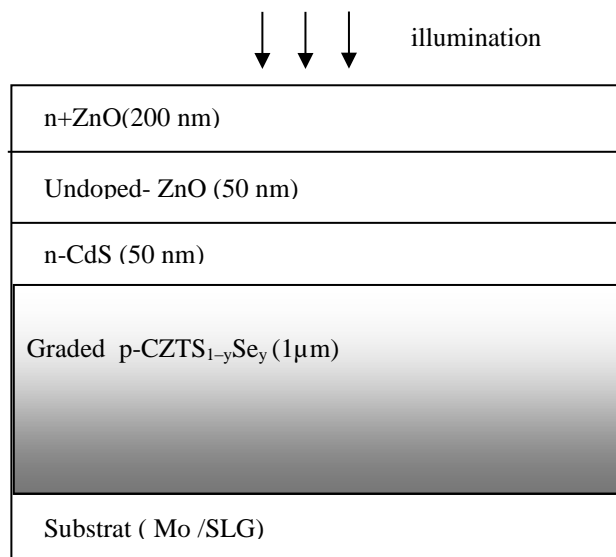


Fig.2. schematic material structure of graded CZTSSe solar cell

Both structures (kesterite and stannite) have been taken into consideration.

Contacts are assumed ohmic or, depending on the focus of the modeling, the metal work function Φ_m (for majority carriers) in SCAPS can be input by the user. However, we can also choose the option “flat bands”. At the contacts a (wavelength dependent) reflection/transmission can be set. The reflection at the back surface has only minor influence on the achievable short-circuit current density (J_{sc}), and these influences only become noticeable if the absorber is chosen to be fairly thin. The only variations in the reported simulations below occur in the composition of the absorber layer. We have used the acronyms: kt-CZTS_{1-y}Se_y for kesterite $\text{CuZnSn}(\text{S}_{1-y}\text{Se}_y)_4$ and st-CZTS_{1-y}Se_y for stannite $\text{CuZnSn}(\text{S}_{1-y}\text{Se}_y)_4$. The rest of the solar cell device and illumination conditions remain untouched. No interface defects or interface-specific properties were added. The CdS and undoped-ZnO layers contain “neutral” defects which provide carriers but do not contribute to the space charge region.

All simulations were run under AM 1.5. The model used in this work has been developed by the author and not adapted from any SCAPS existing example distributed with SCAPS 1D.

3.3. CZTS_{1-y}Se_y absorber layer

It is well known at present that the gradual substitution of S by Se in kesterite and stannite CZTS_{1-y}Se_y affects its structural, electronic, and optical properties. The band-gap changes linearly with (Se) compositions and obeys the Vegard's rule. This is confirmed by Calculated results [20,21,22,23] which agree well with experimental results of various measurement techniques summarized in [5]. We have chosen to describe Eg of CZTS_{1-y}Se_y material by the proposed equations of ref [23] as illustrated in table1.

Table 1. Optical band-gap energy of Kesterite and stannite CZTS_{1-y}Se_y alloys.

absorber	Kesterite CZTS _{1-y} Se _y	Stannite CZTS _{1-y} Se _y
Eg (eV)	$1.505(1 - y) + 0.984y - 0.123y(1 - y)$	$1.308(1 - y) + 0.759y - 0.044y(1 - y)$

When “y” varied gradually from (0 to 1) the composition of the alloy varied linearly from CZTS to CZTSe. from ref [24] as shown in fig.3, the valence band maximum (VBM) of CZTS_{1-y}Se_y alloys is almost linearly down-shifting along with Se composition, and the variation range is very small (~0.15eV); while the conduction band minimum (CBM) of CZTS_{1-y}Se_y alloys is also almost linearly down-shifting along with Se composition, but the variation range are relatively large (~0.35 eV).

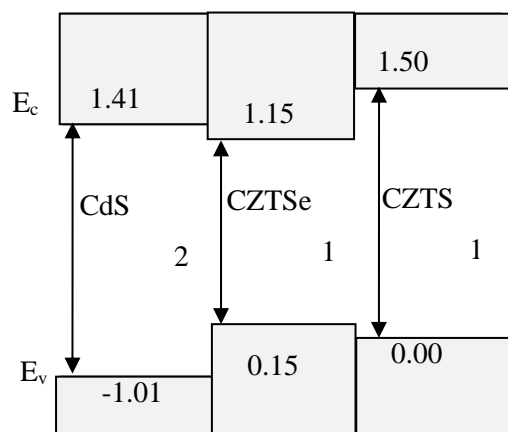


Fig.3. schematic diagram of the band alignment between CdS, CZTS and CZTSe

The conduction and valence band effective density of states, electron and hole thermal velocities, were used from data reported in Ref [25]. The hole mobility of p-CZTS and p-CZTSe

used are 30 and 40 $\text{cm}^2 \text{V}^{-1} \text{s}^{-1}$ respectively, those values were extracted from curve of mobility as function of free-hole concentration ($N_A=2.10^{16}$) [24,25a]. The optical absorption coefficient $\alpha(\lambda)$ of the four absorber layers: kesterite CZTS, kesterite CZTSe, stannite CZTS and stannite CZTSe are determined directly from the complex dielectric function in ref [5]. According to refs [29, 30,31] CdS/CZTSe and CdS/CZTS conduction band offset (CBO) is, respectively, a “spike,” and “cliff”. The CdS CB edge sits, respectively, above that for CZTSe and under that for CZTS. The CBO is the same for both kesterite and stannite, with 0.14 eV difference between the two structures reflected just as a change in the conduction band minimum. In order to model non-radiative recombination (S-R-H) in CZTS_{1-y}Se_y layer, a Gaussian distribution of defects was introduced in the gap and centered in its midpoint as shown in table 2.

Table 2. General layer parameters used as input for SCAPS simulations

Layer Properties at 300° Ks: kesterite ,st: stannite					
layer	CZTS ks/st	CZTSe ks /st	n-CdS	i-ZnO	n+ZnO
thickness (μm)	1.2	1.2	0.05	0.05	0.2
E_g (eV)	1.5 /1.3	1.0/0.76	2.42	3.37	3.37
Electric permittivity	6.5	8.6	10	9	9
Electron affinity (eV)	4.1	4.35	4.2	4.5	4.5
v_{thn} (m/s)	100	100	100	100	100
v_{thp} (m/ s)	30	40	25	25	25
$N_c(\text{cm}^{-3})$	8.1×10^{16}	7.9×10^{17}	2.0×10^{19}	9×10^{18}	2.2×10^{18}
$N_v(\text{cm}^{-3})$	1.5×10^{19}	4.5×10^{18}	1.5×10^{18}	4×10^{18}	1.8×10^{19}
Shallow density (cm^{-3})	1×10^{16}	1×10^{16}	1×10^{17}	1×10^{18}	1×10^{19}
Defect: (a) indicates acceptor and (d) donor[]					
type	(d)/(a)	(d)/(a)	(a)	(a)	(a)
Energy level above EV(eV)	0.40/0.08	0.40/0.08	1.20	1.65	1.65
Density (cm^{-3})	$10^{14}/10^{15}$	$10^{14}/10^{15}$	10^{16}	10^{17}	10^{18}

From what was previously explained: when “y” changes from (0 to 1) the band-gap energy of ks-CZTS_{1-y}Se_y and st-CZTS_{1-y}Se_y changes linearly, respectively, from 1.5 to 0.98 eV and from 1.3 to 0.76 eV. Practically these are the data that have been exploited to tailor and optimize the solar cell. In this work we have tested the effect of grading on the photovoltaic performance of CZTSSe/CdS/ZnO/n+ZnO by simulation and we tried to answer the question: what kind of grading can be useful. Simulation was carried out in both cases kesterite and stannite structure.

4. RESULT AND DISCUSSION

To be able to determine the real effect of grading, simulation results of graded cell should be compared with those of a uniform cell. Solar cells with uniform composition were simulated

by SCAPS. Open circuit voltage (V_{oc}) in mV, density of short circuit current (J_{sc}) in mA/cm^2 , fill factor (FF %) and efficiency (η %) of solar cells of uniform absorber were carried out and illustrated on table.3.

Table 3. properties of kesterite and stannite uniform solar cells by SCAPS

Absorber	V_{oc} (mV)	J_{sc} (mA/cm^2)	FF %	η %
CZTS(ks /st)	1.055 / 0.860	14.11/ 17.12	77.28/ 75.72	11.50/ 11.15
CZTS _{0.8} Se _{0.2} (ks /st)	0.932/ 0.729	15.66/ 18.73	78.46/ 76.63	11.45/ 10.46
CZTS _{0.6} Se _{0.4} (ks /st)	0.826/ 0.615	17.24/ 20.72	78.51/ 76.06	11.17/ 9.69
CZTS _{0.4} Se _{0.6} (ks /st)	0.725/ 0.506	18.88/ 22.68	77.86/ 74.29	10.66/ 8.53
CZTS _{0.2} Se _{0.8} (ks /st)	0.629/ 0.402	20.87/ 24.67	76.35/ 70.94	10.01/ 7.04
CZTSe(ks /st)	0.536/ 0.302	22.81/ 26.66	73.93/ 64.84	9.04/ 5.22

The ratio of “Se” in the absorber material, affects both J_{sc} and V_{oc} of the cell. Higher E_g leads to higher V_{oc} but lower J_{sc} , this is very clear in the two cases, Kesterite and Stannite solar cell. The grading of absorber layer parameters is not the only source of the trade-off between J_{sc} and V_{oc} . Another parameter to be taken into consideration here is the CBO at the contact CZTS_{1-y}Se_y/CdS as shown on fig.4.

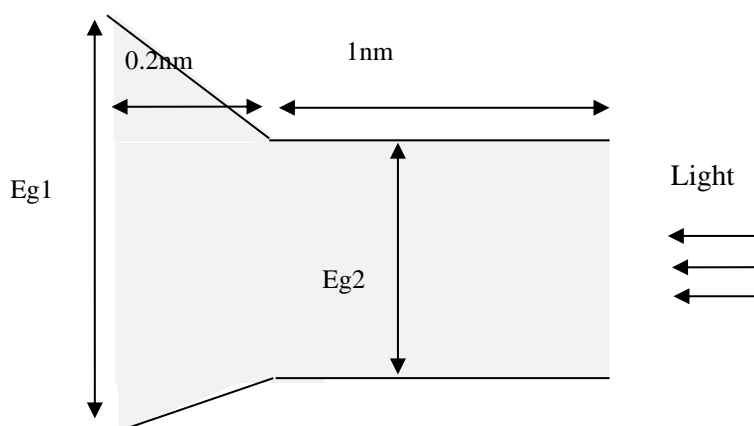


Fig.4. schematic band gap diagram of the optimized compositionally graded CZTS_{1-y}Se_y absorber layer

The CB alignment is “spike-like” at the CZTSSe/CdS interface and “cliff-like” at CZTS/CdS interface. In all that we will discuss later, we assume that “back” means the region near the contact with “Mo” and “front” means the region near the contact with CdS.

4.1 – profile (a)

In profile (a), the absorber layer was fully graded from back to front. In other word, starting with large E_g at the absorber back and finishing with small E_g at the front. We have assumed uniform Ks-CZTSe and St-CZTSe($y=1$) as basic cells with efficiency of, respectively, 9.04 and 5.22% as shown in table3. In order to test the effect of grading, the material composition at back was changed progressively from material of $y=1$ to material of $y=0$ with step of 0.1 while maintaining a fix value of $y=1$ at the front of the absorber layer. The four output parameters V_{oc} , J_{sc} , FF and efficiency of profile (a) are shown in Fig 5.

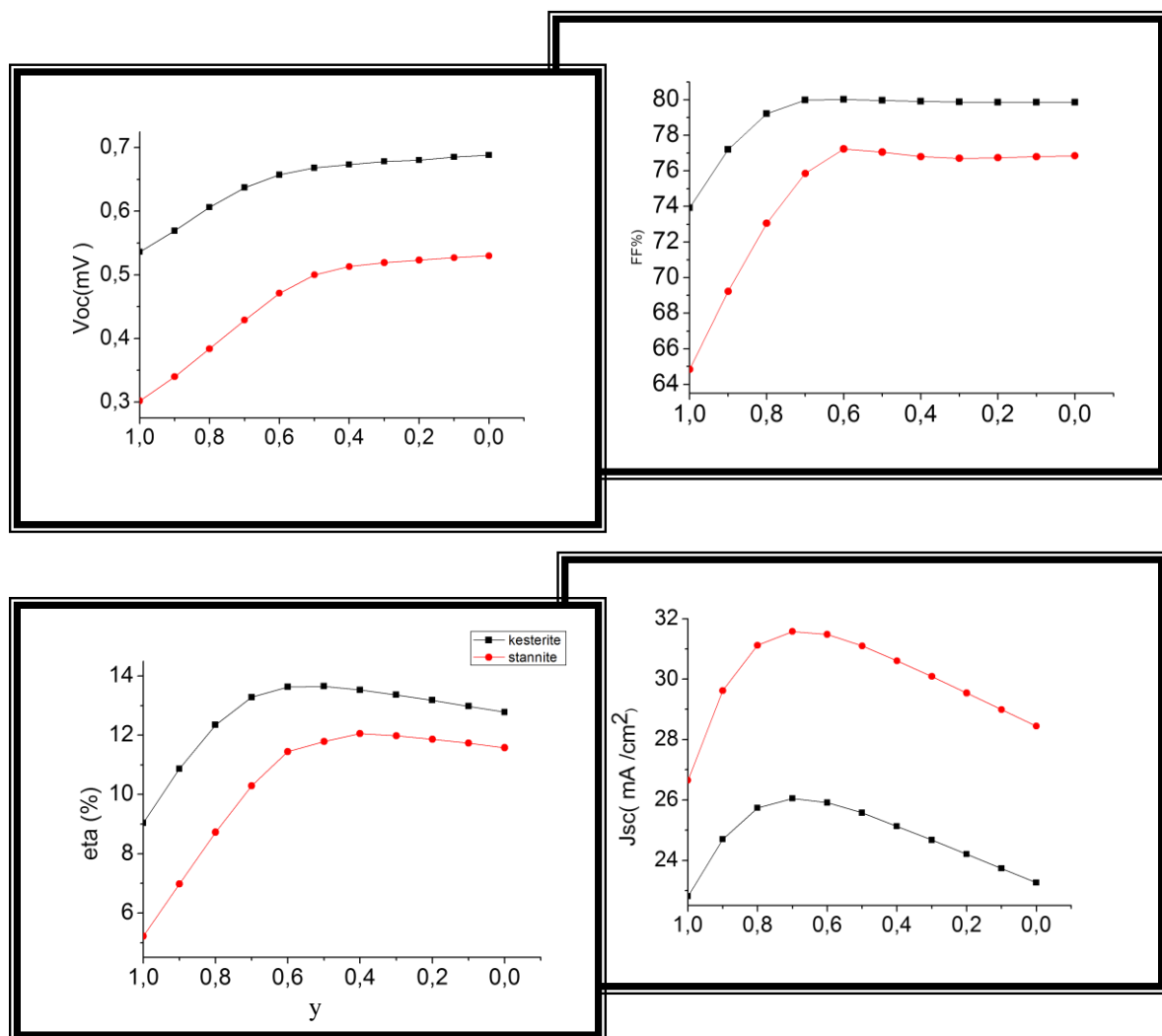


Fig.5. Influence of grading profile (a) on the four parameters, “y” variable at the contact CZTSSe /Mo and maintained equal to “1” at the contact CZTSSe /CdS.

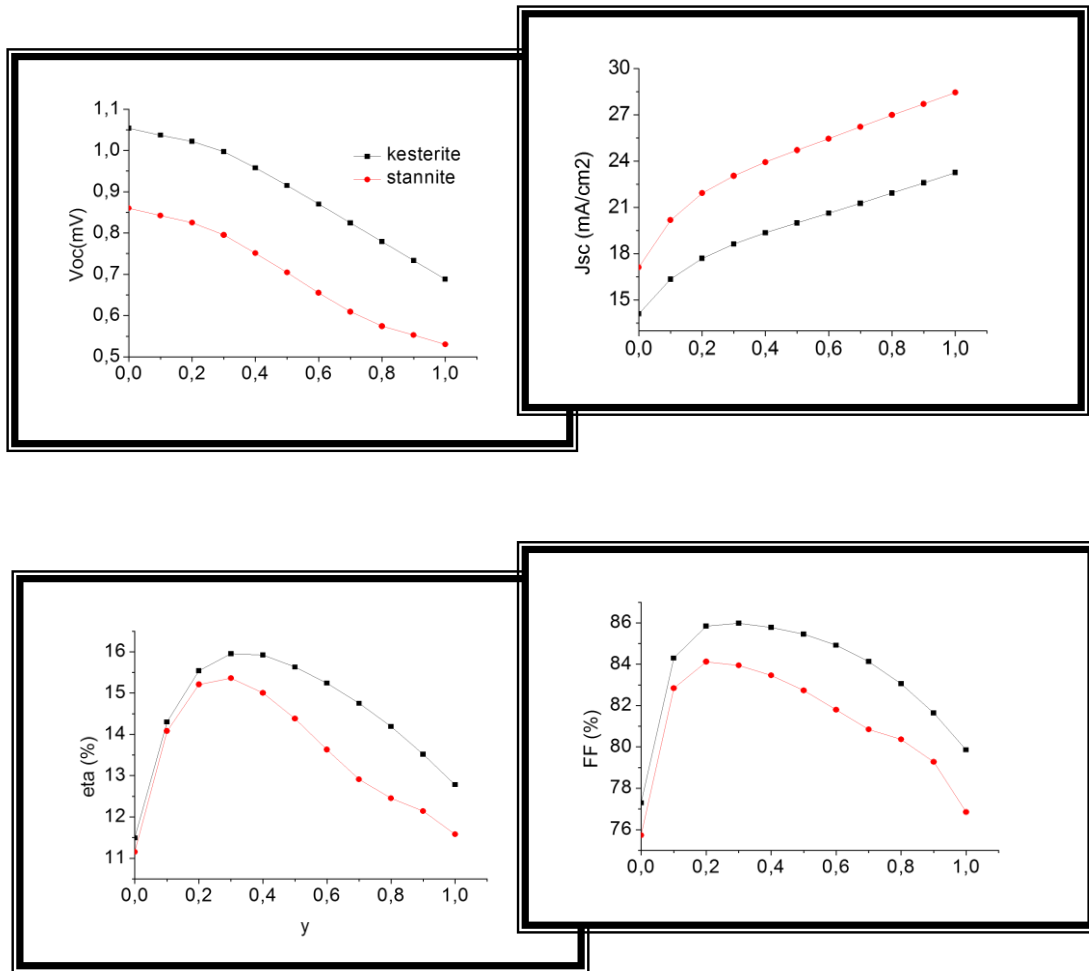


Fig.6. Influence of grading profile (a) on the four parameters, “y” variable at the contact CZTSSe /CdS and maintained =0 at the contact CZTSSe /Mo.

We can remark the same effect of grading on Ks-CZTS_{1-y}Se_y and St-CZTS_{1-y}Se_y cells. In kesterite cell, when “y” changes from (0 to 1), Voc rises linearly from 0.54 to 0.69 mV and Jsc from 22.81 to 23.26 mA /cm² reaching a maximum of 26.05 mA /cm² at y=0.7. The best efficiency (13.65%) is obtained at y = 0.5. In the case of stannite cell, when y changes from (0 to 1), Voc rises linearly from 0.30 to 0.53 mV and Jsc from 26.65 to 28.44 mA /cm² reaching a maximum of 31.58 mA /cm² at y=0.7. The best cell efficiency (12.05%) was obtained at y = 0.4. the open circuit current of St-cell is always more important than that of ks-cell because E_g of St-CZTS_{1-y}Se_y is inferior than that of Kt-CZTS_{1-y}Se_y. it is well known that only photons with energy equal or greater than E_g contribute to current generation.

The profile (a) can be obtained by another strategy. A fix value of y=0 is maintained at absorber back and y changes at front from y=0 to y=1. Here, our basic cells are uniform Ks- CZTS and

uniform St-CZTS with efficiency of 11.50 and 11.15%, respectively (table3). As shown in Fig.6 changing “y” from (0 to1) decrease Voc and increase Jsc of Ks-cell and St-cell linearly. By trade-off between Voc and Jsc, an optimized efficiency is obtained at $y=1$ at absorber back and $y=0.3$ at absorber front. the efficiency reaches 16% and 15.35 % for Ks-cell and St-cell respectively. The best value of FF was obtained at $y= 0.2$ in the tow cells.

4.2 profile (b)

In device with gradual absorber profile (b), the absorber is double graded from front and from back. Here, the basic solar cell was Ks-CZTS and St-CZTS with efficiency of, respectively, 9.04 and 5.22% as shown in table3. It was found that front grading destroys the efficiency as a consequence of the rapid decrease in Jsc and FF. This can be explained by the increase in CBO at the contact with CdS. The third layer acts as barrier prevent electrons to reach the junction. Profile (b) will be effective just in the case of back grading. thus, the absorber was divided only into two layers of 0.2 and 1.0 μm as Fig.4 shows. The composition of the second layer was maintained at $y=1$ ($E_{g2}=E_{g_{CZTS_e}}$). The first layer was graded from $y=0$ at the back of the absorber layer, reaching $y=1$ at the end of this layer. the value of “y” changes toward the back of the first layer. The four parameters of all cells are summarized in Fig7. Voc, Jsc, FF, and the efficiency increase in the same way. The efficiency of Kt-cell and St-cell increases, respectively, from 9.04 to 13.94 and from 5.22 to 11.75 eV. we can remark that using a gradual profile in the first layer is more efficient in st-cell than in ks-cell. In this case another helping factor is added, the creation of back surface field as consequent of the existence of grading at only 0.2 μm .

The absorber layer can be engineered in other strategy to obtain profile (b) with back grading. The composition at the back of the first layer was maintained at $y=0$. the second layer is always uniform but “y” of Ks/St-CZTS_{1-y}Se_y changes in every step. the composition at the front of first layer is the same as the uniform layer (layer 2). In spite of the dramatic reduction in Jsc as shown in curves of Fig 8. This kind of grading gives excellent efficiency. When $y=0.3$ in the second layer, a maximum efficiency of Ks-cell and St-cell, respectively, of 16.65 and 15.77% was obtained when $y=0.3$ and $y=0.2$ respectively. We expect that all preceding discussion can be helpful to predict the real effect of grading in composition of CZTSSe/CdS/ZnO solar cell.

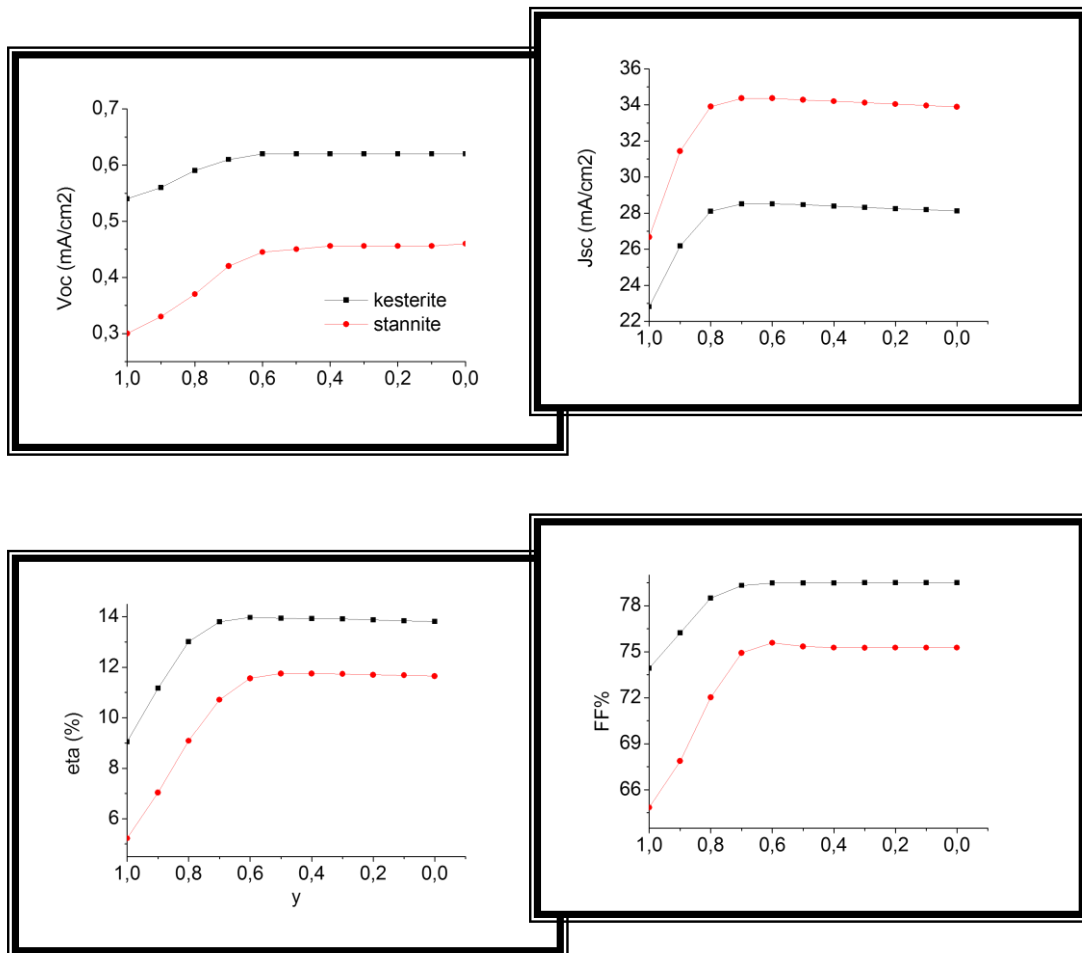


Fig.7. Influence of grading profile (b) on the four parameters, the variation of “y” is at the contact CZTSSe /Mo in the first layer, “y” is maintained equal to “1” in the second layer.

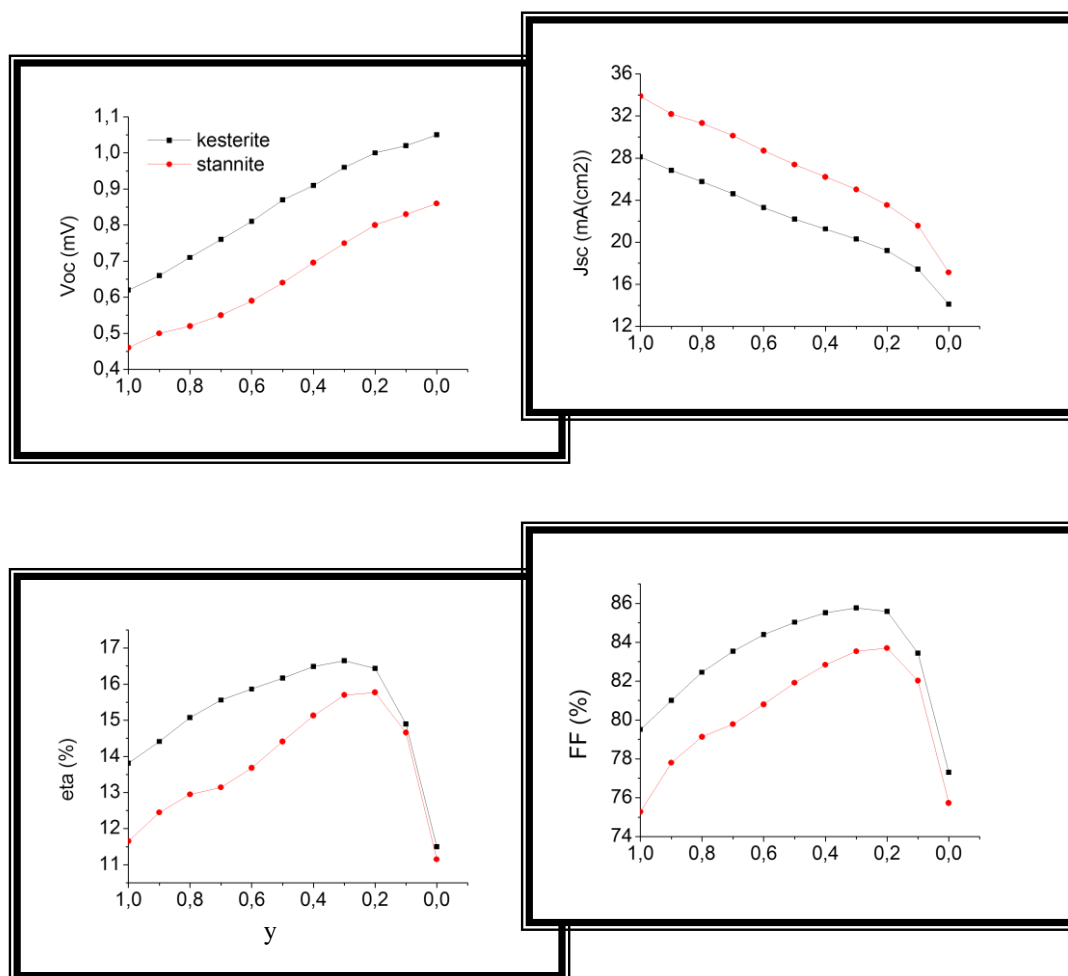


Fig.8. Influence of grading profile (b) on the four parameters, “y” is maintained equal to “0” at the contact CZTSSe /Mo and variable in the second layer.

5. CONCLUSION

The goal of this work is to increase the efficiency of CZTSSe/CdS/ZnO solar cell, depending on the idea that substituting sulfur atoms by selenium atoms in CZTSSe absorber layer causes a change in the gap. The gradual substitution leads to a gradual absorber layer gap. The influence of Tow grading profile on the efficiency of CZTSSe cell was investigated: fully graded profile (a) and double graded profile (b). Simulation was carried out in both structures kesterite and stannite using the simulation package, SCAPS 1D. in profile (a) We have assumed uniform Ks-CZTSSe($y=1$) and St-CZTSSe($y=1$) as basic cells then absorber layer was fully graded. The efficiency gradually improved until it reaches 16 and 15.35 % for Ks-cell and St-cell respectively. In profile (b) the basic uniform cell is Ks-CZTS($y=0$) and St-CZTS($y=0$). Front grading had a disruptive effect on solar cell parameters, in contrary back grading

ameliorates significantly all cell parameters. The efficiency gradually improved until it reaches 16.65 and 15.77%eV for Ks-cell and St-cell respectively. As a final word, we can say that grading the absorber layer gap enhance cell efficiency in a satisfactory way, if we follow a certain strategy that takes in consideration CdS/CZTS conduction band offset.

6. ACKNOWLEDGEMENTS

The author would like to acknowledge gratefully Marc Burgelman from ELIS, University of Gent for his precious instructions.

7. REFERENCES

- [1] C.M. Fella, Y. E. Romanyuk, A.N. Tiwari, *Solar Energy Materials & Solar Cells* 119 (2013) 276–277.
- [2] X. Song, X. Ji, M. Li, W. Lin, X. Luo, and H. Zhang. Hindawi Publishing Corporation *International Journal of Photoenergy*. Volume 2014, Article ID 613173.
- [3] K.ito, *Copper Zinc Tin Sulfide-Based Thin-Film Solar Cells*, first edition 2015 John Wiley & Sons, Ltd. ISBN: 978-1-118-43787-2
- [4] P.A. Fernandes, P.M.P. Salome', A.F. da Cunha, *Thin Solid Films* 517 (7) (2009) 2519–2523.
- [5] S. Das, K. C. Mandal, *Materials Research Bulletin* 57 (2014) 135–139.
- [6] G. Altamura & all, *Journal of Renewable and Sustainable Energy* 6 (2014), 011401;
- [7] K. Ito & T. Nakazawa, (1988) *Japanese Journal of Applied Physics*, 27, 2094–2097.
- [8] M. Green, K. Emery, Y. Hishikawa, W. Warta & E. Dunlop, (2014) Solar cell efficiency tables (version 43). *Progress in Photovoltaics*, 22, 1–9.
- [9] Wang, W., Winkler, M.T., Gunawan, O., Gokmen, T., Todorov, T.K., Zhu, Y. & Mitzi, D.B. (2013) *Advanced Energy Materials*, published online November 2013, doi: 0.1002/aenm.201301465 (2013)
- [10] T. Eguchi, T. Maki, S.Tajima, T.Ito and T. Fukano. Technical Digest, 21st International Photovoltaic Science and Engineering Conference, Fukuoka, November 2011: 4D-3P-24.
- [11] W. Shockley, H.J. Queisser, *J. Appl. Phys.*, 32 (1961) 510-519.
- [12] K. Woo, Y. Kim, W. Yang, K. Kim, I. Kim, Y. Oh1, J. Y. Kim & J Moon, (2013) *SCIENTIFIC REPORTS* | 3: 3069 | DOI: 10.1038/srep03069
- [13] S. J. Fonash; *Solar Cell Device, Physics*, ACADEMIC PRESS ,1981
- [14] C. Snowden, *Introduction to semiconductor device modeling*, World Scientific, 1986.

- [15] M. Burgelman, J. Marlein, Proceedings of the 23rd European Photovoltaic Conference, Valencia, Spain (2008) 2151-2155.
- [16] A. Morales-Acevedo, Energy Procedia 2 (2010) 169–176
- [17] M. Burgelman, P. Nollet and S. Degrave, Thin Solid Films, (2000) 361-362, 527-532.
- [18] E. A. Lunda and M.A. Scarpulla, Proc. of SPIE Vol. 8620 862015- Downloaded From: <http://proceedings.spiedigitallibrary.org/> on 06/28/2013
- [19] B. Shin, O. Gunawan, Y. Zhu, N. A. Bojarczuk, S. J. Chey and S. Guha, Prog. Photovolt: Res. Appl. 2013; 21:72–76
- [20] Chen, S., Gong, X. G., Walsh, A. & Wei, S. H. (2009), *Applied Physics Letters*, 94, 041903-1-3.
- [21] J.Paier, R.Asahi, A. Nagoya. &G. Kresse, (2009), *Physical Review B*, 79,115126-1-8.
- [22] Chen, S., Gong, X. G., Walsh, A. & Wei, S. H. (2009), *Physical Review B*, 79, 165211-1-10.
- [23]Z-Y. Zhao, Q-L. Liu, X. Zhao, Journal of Alloys and Compounds (2014), jallcom.2014.08.213
- [24] Ingrid Repins, Nirav Vora, Carolyn Beall, Su-Huai Wei, Yanfa Yan, Manuel Romero, Glenn Teeter, Hui Du, Bobby To, Matt Young, and Rommel Noufi, Materials Research Society Spring Meeting San Francisco, California (2011), NREL/CP-5200-51286
- [25] Persson, C., Journal of Applied Physics 107(5), 053710 (2010). (a virifier)
- [26] Nagaoka, A., Yoshino, K., Taniguchi, H., Taniyama, T. & Miyake, H. (2012). Journal of Crystal Growth, 341, 38–41.
- [27] Wibowo, R. A., Lee, E. S., Munir, B. & Kim, K. H. (2007). Physica Status Solidi A, 204, 3373–3379.
- [28] J. He, L. Sun, S. Chen, Y. Chen, P. Yang, J. Chu, Journal of Alloys and Compounds 511 (2012) 129–132.
- [29] S. Chen, A. Walsh, J. Yang, X. G. Gong, L. Sun, P. Yang, J. Chu, and S. Wei, PHYSICAL REVIEW B 83, 125201 (2011)
- [30] A.Nagoya, R. Asahi and G.Kresse, Journal of Physics: Condensed matter 23(40), 404203 (2011).(verf)
- [31] R.Haight, A. Barkhouse, O. Gunawan, B. Shin, M. Copel, M. Hopstaken, and D.B Mitzi, Applied Physics Letters 98(25), 253502 (2011).

How to cite this article:

Messei N. Influence of absorber layer gradual gap profile on $\text{Cu}_2\text{ZnSn}(\text{S}_{1-y}\text{Se}_y)_4$ solar cell efficiency: numerical study. J. Fundam. Appl. Sci., 2021, 13(1), 385-399.